

# Heavy-quark spin symmetry partners of the $X(3872)$ revisited

V. Baru<sup>a,b</sup>, E. Epelbaum<sup>a</sup>, A. A. Filin<sup>a</sup>, C. Hanhart<sup>c</sup>, Ulf-G. Meißner<sup>c,d</sup>, A. V. Nefediev<sup>b,e,f</sup>

<sup>a</sup>*Institut für Theoretische Physik II, Ruhr-Universität Bochum, D-44780 Bochum, Germany*

<sup>b</sup>*Institute for Theoretical and Experimental Physics, B. Chermushkinskaya 25, 117218 Moscow, Russia*

<sup>c</sup>*Forschungszentrum Jülich, Institute for Advanced Simulation, Institut für Kernphysik and Jülich Center for Hadron Physics, D-52425 Jülich, Germany*

<sup>d</sup>*Helmholtz-Institut für Strahlen- und Kernphysik and Bethe Center for Theoretical Physics, Universität Bonn, D-53115 Bonn, Germany*

<sup>e</sup>*National Research Nuclear University MEPhI, 115409, Kashirskoe highway 31, Moscow, Russia*

<sup>f</sup>*Moscow Institute of Physics and Technology, 141700, 9 Institutsky lane, Dolgoprudny, Moscow Region, Russia*

---

## Abstract

We revisit the consequences of the heavy-quark spin symmetry for the possible spin partners of the  $X(3872)$ . We confirm that, if the  $X(3872)$  were a  $D\bar{D}^*$  molecular state with the quantum numbers  $J^{PC} = 1^{++}$ , then in the strict heavy-quark limit there should exist three more hadronic molecules degenerate with the  $X(3872)$ , with the quantum numbers  $0^{++}$ ,  $1^{+-}$ , and  $2^{++}$  in line with previous results reported in the literature. We demonstrate that this result is robust with respect to the inclusion of the one-pion exchange interaction between the  $D$  mesons. However, this is true only if all relevant partial waves as well as particle channels which are coupled via the pion-exchange potential are taken into account. Otherwise, the heavy-quark symmetry is destroyed even in the heavy-quark limit. Finally, we solve the coupled-channel problem in the  $2^{++}$  channel with nonperturbative pions beyond the heavy-quark limit and, contrary to the findings of previous calculations with perturbative pions, find for the spin-2 partner of the  $X(3872)$  a significant shift of the mass as well as a width of the order of 50 MeV.

*Keywords:* exotic hadrons, charmonium, chiral dynamics, effective field theory

---

## 1. Introduction

In the previous decade, lots of states were found experimentally in the heavy quarkonium mass range that did not at all fit into the scheme predicted by the until then very successful constituent quark model—for a review see, *e.g.*, Refs. [1, 2]. Amongst those many states, the  $X(3872)$  is special not only because it was the first such an extraordinary state discovered—it was first seen by the Belle Collaboration in 2003 [3]—but also because it resides extremely close to the  $D^0\bar{D}^{*0}$  threshold. Indeed, with a mass  $M_X = 3871.68 \pm 0.17$  MeV [4] its binding energy is as small as

$$E_X = m_0 + m_{*0} - M_X = 0.12 \pm 0.30 \text{ MeV}, \quad (1)$$

where  $m_0$  ( $m_{*0}$ ) denotes the mass of the  $D^0$  ( $D^{*0}$ ) meson [4]. Thus it has been regarded as one of the most promising candidates for a hadronic molecule, which may be either an  $S$ -wave bound state [5–10] or a virtual state in the  $D\bar{D}^*$  system [11]; both possibilities are

in line with its quantum numbers, which were determined by the LHCb Collaboration to be  $J^{PC} = 1^{++}$  [12]. Other models exist in addition to the hadronic molecule interpretation, which include  $\chi_{c1}(2P)$  [13]—the first radial excitation of the  $P$ -wave charmonium  $\chi_{c1}(1P)$ ,—a tetraquark [14], a mixture of an ordinary charmonium and a hadronic molecule [15, 16], or a state generated in the coupled-channel dynamical scheme [17, 18].

One of the celebrated theoretical tools used in studies of hadronic states with heavy quarks is the Heavy-Quark Spin Symmetry (HQSS). HQSS is based on the observation that for  $\Lambda_{\text{QCD}}/m_Q \rightarrow 0$ , with  $m_Q$  denoting the quark mass, the strong interactions in the system are independent of the heavy quark spin. Then, although in case of the charm quark  $\Lambda_{\text{QCD}}/m_c \simeq 0.2$  is sizable and one expects non-negligible corrections to the strict symmetry limit, constraints from HQSS can still provide a valuable guidance also in the charm sector and in particular for the  $X(3872)$  [19]. Meanwhile it was demonstrated in Ref. [20] that the consequences of HQSS are very different for the different scenarios for the  $X$ . It is therefore crucial to refine the quantitative predictions for the various scenarios. In this work we focus on a hypothesis that the  $X(3872)$  is a molecular state and investigate the consequences that arise from HQSS as well as its leading violations. In particular, in Refs. [21–23] the spin partners of the isovector states  $Z_b^+(10610)$  and  $Z_b^+(10650)$  were investigated in the molecular picture and several degenerate states were predicted. Similarly, it was argued in Refs. [24, 25] that one should expect a shallow bound state in the  $D^*\bar{D}^*$  channel with the quantum numbers  $J^{PC} = 2^{++}$  — the molecular partner of the  $X(3872)$ . In Ref. [26], based on an effective field theory with perturbative pions (X-EFT), the width of this state was estimated to be as small as a few MeV.

In all mentioned studies as well as in this work an assumption is made for the dominant molecule component of the wave functions of the states and observable implications of this assumption are investigated. In reality one can expect that there is an admixture of different components too. However, given the current quality of the data it appears unclear whether or not the effect of the subdominant components can be identified reliably within a given state. An exploratory study of the possible impact of genuine quarkonium states on the formation of the molecular spin multiplets is presented in Ref. [27]. In the future it would certainly be of interest to combine the insights presented in this paper with the ideas of Ref. [27].<sup>1</sup>

In this paper we refine further the implications of HQSS for the  $X(3872)$  and its partners in the molecular picture and critically re-examine the findings of the above mentioned papers. In particular, we investigate in detail the implications of HQSS for the spin partners of the  $X(3872)$  with and without one pion exchange (OPE). We adapt the methods of Ref. [23] to isoscalar states in the presence of OPE, with a special emphasis on the renormalisation to leading order in the heavy quark expansion. Furthermore, we go beyond the heavy-quark limit to demonstrate that the scales emerging in the coupled-channel approach due to the nonperturbative treatment of the pions generate a significant width of the  $2^{++}$  spin partner of the  $X(3872)$  as well as a sizeable shift of its mass.

---

<sup>1</sup>Note that according to Ref. [28] it might well be insufficient to include just a single quarkonium state in each channel.

## 2. Pionless theory—contact interactions only

### 2.1. Strict heavy-quark limit: Spin partners of the $X(3872)$

Although pions play an important role in realistic calculations of the spin partners, as we shall demonstrate below, it is instructive to start from a simple analytically solvable model with the only  $S$ -wave contact interactions. The methods applied in this section to the isoscalar states in the charmonium sector are similar to those used in Ref. [23] for isovector states in the bottomonium sector. In this subsection we discuss the results at leading order (LO) in the heavy-quark expansion which we call the strict HQSS limit. In this case, the masses of the  $D$  and  $D^*$  are identical. The corrections due to the finite  $D^*$ - $D$  mass splitting will be discussed in subsection 2.2.

The basis states introduced in Ref. [24] read

$$\begin{aligned}
0^{++} &: \{D\bar{D}(^1S_0), D^*\bar{D}^*(^1S_0)\}, \\
1^{+-} &: \{D\bar{D}^*(^3S_1, -), D^*\bar{D}^*(^3S_1)\}, \\
1^{++} &: \{D\bar{D}^*(^3S_1, +)\}, \\
2^{++} &: \{D^*\bar{D}^*(^5S_2)\},
\end{aligned} \tag{2}$$

where the individual partial waves are labelled as  $^{2S+1}L_J$  with  $S$ ,  $L$ , and  $J$  denoting the total spin, the angular momentum, and the total momentum of the two-meson system, respectively. We define the C-parity eigenstates as

$$D\bar{D}^*(\pm) = \frac{1}{\sqrt{2}} (D\bar{D}^* \pm D^*\bar{D}), \tag{3}$$

which comply with the convention<sup>2</sup> for the C-parity transformation  $\hat{C}\mathcal{M} = \bar{\mathcal{M}}$ .

In this basis and for a given set of quantum numbers  $\{JPC\}$ , the leading-order EFT potentials  $V_{\text{LO}}^{(JPC)}$ , which respect heavy-quark spin symmetry, read [24, 30, 31]

$$V_{\text{LO}}^{(0^{++})} = \begin{pmatrix} C_{0a} & -\sqrt{3}C_{0b} \\ -\sqrt{3}C_{0b} & C_{0a} - 2C_{0b} \end{pmatrix}, \tag{4}$$

$$V_{\text{LO}}^{(1^{+-})} = \begin{pmatrix} C_{0a} - C_{0b} & 2C_{0b} \\ 2C_{0b} & C_{0a} - C_{0b} \end{pmatrix}, \tag{5}$$

$$V_{\text{LO}}^{(1^{++})} = C_{0a} + C_{0b}, \tag{6}$$

$$V_{\text{LO}}^{(2^{++})} = C_{0a} + C_{0b}, \tag{7}$$

where  $C_{0a}$  and  $C_{0b}$  are two independent low-energy constants.

The generic matrix integral equation for the scattering amplitude  $a^{(JPC)}(p, p')$  reads

$$a^{(JPC)}(p, p') = V^{(JPC)}(p, p') - \int dk k^2 V^{(JPC)}(p, k) G(k) a^{(JPC)}(k, p'), \tag{8}$$

---

<sup>2</sup> Notice that a different convention for the C-parity operator was used in Ref. [24]. As a consequence, the off-diagonal transitions of  $V_{\text{LO}}^{(0^{++})}$  in Ref. [24] have different sign as compared to Eq. (4), see also Sec. VI A in Ref. [29] for further details of our convention.

and it simplifies considerably in the strict HQSS limit if only the leading-order contact interactions (4)-(7) are included. Here  $G(k)$  denotes the matrix of the propagators of the heavy meson-antimeson pair in the intermediate state. In the single-channel case—see Eqs. (6) and (7)—it reads

$$G(k) = \frac{1}{k^2/\bar{m} - E - i0} \quad (9)$$

while for coupled channels—see Eqs. (4) and (5)— $G(k)$  is a  $2 \times 2$  diagonal matrix with both nonzero elements given by Eq. (9). Here we used that in the strict HQSS limit the  $D^*$ - and  $D$ -meson masses  $m_*$  and  $m$ , respectively, coincide,  $\bar{m} = m_* = m$ . For the quantum numbers  $1^{++}$  and  $2^{++}$  Eq. (8) reduces to a single equation with the solution

$$a^{-1} = C_0^{-1} + \bar{m} \int dk \frac{k^2}{k^2 - \bar{m}E - i0}, \quad (10)$$

where  $C_0 = C_{0a} + C_{0b}$ . The poles appear at the energies where the inverse amplitude,  $a^{-1}$ , vanishes. Accordingly, the value of the low-energy constant  $C_0$  can be fixed from the binding energy of the  $X(3872)$  (denoted below as  $E_X$ ), used as input. Conversely, the binding energy in the  $2^{++}$  channel,  $E_{X_2}$ , can be extracted from this equation, given that  $C_0$  is known. Clearly,  $E_{X_2} = E_X$  in the strict HQSS limit.

As shown in Refs. [19, 21–23, 32], in the heavy-quark limit, one can predict more states with the same binding energy. To this end, one can apply a unitary transformation [23], defined as

$$U = \begin{pmatrix} \cos \phi & \sin \phi \\ -\sin \phi & \cos \phi \end{pmatrix}, \quad (11)$$

to the matrix bound-state Eq. (8) for the  $0^{++}$  and  $1^{+-}$  states. It is easy to see then that, taking  $\phi = -\pi/6$  and  $\phi = \pi/4$  for the  $0^{++}$  and  $1^{+-}$  potentials defined in Eqs. (4) and (5), respectively, one arrives for both quantum numbers at the diagonalised potential

$$\tilde{V}^{(JPC)} = UV^{(JPC)}U^\dagger = \begin{pmatrix} C_0 & 0 \\ 0 & C'_0 \end{pmatrix}, \quad (12)$$

where  $C_0 = C_{0a} + C_{0b}$  and  $C'_0 = C_{0a} - 3C_{0b}$ . Therefore, the poles in both channels are now defined from the equation

$$\det \left[ 1 + \int dk k^2 \tilde{V}^{(JPC)} G(k) \right] = 0, \quad (13)$$

where the propagator matrix is unchanged under rotations (11),  $UG(k)U^\dagger = G(k)$ , since in the strict HQSS limit it is proportional to the unit matrix. Equation (13) has two solutions corresponding to the two different linear combinations of the low-energy constants; one of them,  $C_0$ , is the same for all quantum numbers, including  $1^{++}$  and  $2^{++}$  considered before—see Eq. (10). Therefore the coupled-channel problem defined by Eqs. (4)-(9) in the strict HQSS limit splits into disentangled equations which possess two decoupled solutions,

$$E_X^{(0)} = E_{X_2}^{(0)} = E_{X_1}^{(0)} = E_{X_0}^{(0)} \quad \text{and} \quad E_{X'_0}^{(0)} = E_{X'_1}^{(0)}, \quad (14)$$

where  $E_{X_0}^{(0)}$ ,  $E_{X_1}^{(0)}$ , and  $E_{X_2}^{(0)}$  stand for the binding energies of the spin-0, spin-1, and spin-2 partners of the  $X(3872)$  in the strict heavy-quark limit, respectively, defined by the combination of the low-energy constants  $C_0$  while  $E_{X'_0}^{(0)}$  and  $E_{X'_1}^{(0)}$  label the binding energies of the two additional partner states defined by the low-energy constant  $C'_0$ —see Eq. (12)—if the potential  $C'_0$  is strong enough to bring about bound states.

In summary, in the strict HQSS limit the state  $X(3872)$  should have three degenerate spin partner states with the quantum numbers  $0^{++}$ ,  $1^{+-}$ , and  $2^{++}$ , all of them being isoscalar states, like the  $X(3872)$  itself. In addition, to these four degenerate states, there might exist two further states with the quantum numbers  $0^{++}$  and  $1^{+-}$  with a binding energy governed by the other combination of the low-energy constants,  $C'_0$ . These additional states cannot be predicted from the mass of the  $X(3872)$  and they require additional experimental input. These findings are in line with those reported in Ref. [19].

## 2.2. Inclusion of HQSS breaking corrections

Corrections to the HQSS limit at leading order in  $\Lambda_{\text{QCD}}/m_c$  give rise to the known  $D^*-D$  mass splitting. For convenience, we define the quantities

$$\delta = m_* - m = 141 \text{ MeV}, \quad \bar{m} = (3m_* + m)/4 = 1973 \text{ MeV} \quad (15)$$

and find for the reduced masses of the  $D\bar{D}$ ,  $D\bar{D}^*$ , and  $D^*\bar{D}^*$  pairs to leading order in  $\delta$

$$2\mu = \bar{m} - \frac{3}{4}\delta, \quad 2\mu_* = \bar{m} - \frac{\delta}{4}, \quad 2\mu_{**} = \bar{m} + \frac{1}{4}\delta, \quad (16)$$

respectively.

We start with the uncoupled channels corresponding to the quantum numbers  $1^{++}$  and  $2^{++}$ . If, as explained above, the low-energy constant  $C_0$  is fixed from the binding energy of the  $X(3872)$  (*cf.* Eq. (10)), then for its  $2^{++}$  partner we have the equation

$$0 = 2\mu_* \int dk \frac{k^2}{k^2 + \gamma_X^2 - i0} - 2\mu_{**} \int dk \frac{k^2}{k^2 + \gamma_{X_2}^2 - i0}, \quad (17)$$

where the binding momenta are related to the respective binding energies as

$$\gamma_X^2 = 2\mu_* E_X, \quad \gamma_{X_2}^2 = 2\mu_{**} E_{X_2}, \quad (18)$$

and the binding energies are now defined with respect to the relevant thresholds, namely

$$E_X = m + m_* - M_X, \quad E_{X_2} = 2m_* - M_{X_2}. \quad (19)$$

The integrals in Eq. (17) are linearly divergent and need to be regularised, for example, by a sharp cut-off in momentum,  $k < \Lambda$ . Then, dropping all terms which vanish in the limit  $\Lambda \rightarrow \infty$  and retaining only the leading-order terms in  $\delta$ , we find that

$$\gamma_{X_2} = \left(1 - \frac{\delta}{2\bar{m}}\right) \gamma_X + \frac{\delta}{\pi\bar{m}}\Lambda + \dots, \quad (20)$$

where the ellipsis stands for the small corrections of the order  $O(\gamma_X^2/\Lambda)$  and  $O(\delta^2\Lambda/\bar{m}^2)$ . Equation (20) relates the binding momentum of the  $X_2$  bound state to the binding momentum of the  $X(3872)$  where the latter is treated as input which fixes the strength of the

contact potential  $C_0$ . We therefore see that at order  $O(\delta)$  an additional counter term is necessary to render the result for the mass of the  $J = 2$  partner of the  $X(3872)$  well defined.

The value of the counter term may be estimated by associating  $\Lambda$  with the mass scale related to the pionic degrees of freedom which are integrated out in the contact theory. Alternatively one may argue that  $\Lambda$  should be of order of the typical hadronic scale 1 GeV. Accordingly, the cut-off-dependent term in Eq. (20) may be estimated to range between 3 and 23 MeV for  $\Lambda = m_\pi$  and  $\Lambda = 1$  GeV, respectively. This uncertainty is to be compared with the value of the binding momentum  $\gamma_X$ . To estimate the latter in the isospin limit for the  $D$ -meson masses we consider two alternative assumptions: (i) the binding energy  $E_X$  takes the value quoted in Eq. (1)—this gives  $\gamma_X \approx 15$  MeV—and (ii) the mass of the  $X$  coincides with the experimental one such that  $E_X = 2\bar{m} - M_X \approx 4.2$  MeV, which leads to  $\gamma_X \approx 89$  MeV. We conclude therefore that from the effective theory with only  $S$ -wave contact interactions the  $X_2$  state is expected to lie within a few MeV below the  $D^*\bar{D}^*$  threshold.

It is straightforward to check that similar cut-off-dependent corrections induced by the  $D^*-D$  mass difference appear in the channels with the quantum numbers  $0^{++}$  and  $1^{+-}$ . In addition, as soon as the  $D^*-D$  mass difference is considered, the propagator matrix is not proportional to the unit matrix anymore and thus the product of the potential and the propagator cannot be diagonalised. As a result, the poles which appear for these two quantum numbers are determined by both low-energy constants  $C_0$  and  $C'_0$ —see Eq. (12)—simultaneously. Accordingly, the binding energies in the  $0^{++}$  and  $1^{+-}$  channels are no longer equal to that of the  $X(3872)$ , *cf.* Eq. (14). In order to proceed let us *assume* that there exists a  $1^{+-}$  bound state near the  $D\bar{D}^*$  threshold, which we label as  $X_1$ . Then both low-energy constants  $C_0$  and  $C'_0$  can be determined independently using the binding momenta  $\gamma_{X_1}$  and  $\gamma_X$  of the  $X_1$  and the  $X(3872)$  as input. As a consequence, the binding momenta of the other  $1^{+-}$  and  $0^{++}$  states can be predicted analytically from a coupled-channel approach. It should be stressed, however, that the role played by the coupled-channel effects depends on the interplay of the splitting  $\delta$  and a typical binding energy of the spin partner states  $E_B$ . Had the relevant relation between the scales been  $\delta \ll E_B$ , then the binding energies discussed in the previous section—see Eq. (14)—would have acquired only small corrections, perturbative in  $\delta$ . However, in the realistic case the situation is opposite,  $\delta \gg E_B$ —see Eq. (15) for the physical value of  $\delta$ —which calls for a different expansion for the coupled-channel equations. In particular, now  $\sqrt{m\delta}$  can be treated as a large parameter, and the expansion can be performed in powers of the small ratio  $\gamma_B/\sqrt{m\delta}$ , where  $\gamma_B$  is the binding momentum corresponding to the binding energy  $E_B$  in the given channel [23]. For example, by an explicit calculation one arrives at

$$\gamma_{X'_1} = \left(1 - \frac{\delta}{2\bar{m}}\right) \gamma_{X_1} + \frac{\Lambda\delta}{\pi\bar{m}} - \frac{(\gamma_{X_1} - \gamma_X)^2}{\sqrt{m\delta}} + i \frac{(\gamma_{X_1} - \gamma_X)^2}{\sqrt{m\delta}} + \dots \quad (21)$$

for the binding momentum of the other  $1^{+-}$  state, residing near the  $D^*\bar{D}^*$  threshold and here referred to as  $X'_1$ . This result is remarkable in two respects. First, states belonging to different HQSS multiplets—see Eq. 14—are strongly mixed by the coupled-channel dynamics, so that the binding energy of the  $1^{+-}$   $D^*\bar{D}^*$  state  $X'_1$  depends now on both input parameters  $\gamma_X$  and  $\gamma_{X_1}$ . Second, the binding momentum  $\gamma_{X'_1}$  acquires an imaginary part and so does the binding momentum  $\gamma_{X'_0}$  of the  $X'_0$  state (the spin-0 state near the  $D^*\bar{D}^*$  threshold). This is a reflection of the fact that beyond the strict HQSS limit in the systems with the quantum numbers  $0^{++}$  and  $1^{+-}$  transitions  $D^*\bar{D}^* \rightarrow D\bar{D}^{(*)}$  are possible due to coupled

channels already in the pionless theory. It is important to notice that such imaginary parts are controlled by unitarity and therefore they are cut-off-independent to leading order—see Eq. (21). The inclusion of the OPE interaction brings about additional partial waves in all channels and makes the transitions  $D^*\bar{D}^* \rightarrow D\bar{D}^{(*)}$  possible for the quantum number  $2^{++}$  as well, so that  $\gamma_{X_2}$  becomes complex too—in other words, also the state  $X_2$  acquires a finite width. Meanwhile, as is demonstrated by the calculations described below, OPE does not spoil the property that the width of the spin-partner state shows only a rather mild cut-off dependence, which makes it possible to treat the broadening of  $\Gamma_{X_2}$  found in the calculations with nonperturbative pions as a reliable prediction of the approach.

### 3. Contact plus OPE interactions

It is often claimed that OPE plays a crucial role for the formation of the  $X(3872)$ —the existence of the latter was even predicted based on a model that contained OPE only [8]. We shall therefore investigate now the possible role of OPE from an effective field theory point of view. Since OPE in leading order is in line with HQSS, its inclusion does not destroy the multiplet structure discussed above. However, as we shall demonstrate below, this is only true if both coupled channels and  $D$  waves are included properly. Before studying this issue for the full, nonperturbative system, for illustrative purposes, we start with a discussion of the OPE contributions to one-loop order. This is sufficient to make the mentioned features apparent from the divergence structure of the amplitudes.

#### 3.1. Strict heavy-quark limit: Renormalisation to one loop

In this subsection we study the leading divergences of the one-loop diagrams which stem from two iterations of the OPE potential. We are going to demonstrate that, in the heavy-quark limit, the coefficients in front of the leading divergences in the  $D\bar{D}^* \rightarrow D\bar{D}^*$  ( ${}^3S_1$  partial wave) and  $D^*\bar{D}^* \rightarrow D^*\bar{D}^*$  ( ${}^5S_2$  partial wave) transition amplitudes coincide only if both  $D\bar{D}^*$  and  $D^*\bar{D}^*$  intermediate states are considered and all partial wave are kept in the calculation. The corresponding set of diagrams is shown in Fig. 1, where the upper row is for the  $D\bar{D}^* \rightarrow D\bar{D}^*$  transition while the lower row is for the  $D^*\bar{D}^* \rightarrow D^*\bar{D}^*$  transition. For convenience, we adopt the following convention: the meson floating along the upper line in each diagram is labelled by index 1 while the meson in the lower line is labelled by index 2. Also, particles in the final state are marked with a prime while particles in the intermediate state are marked with a double prime.

In order to extract the leading divergences it is sufficient to retain only the loop momentum, denoted as  $\mathbf{l}$ , in each vertex. Then, for example, the  $D^* \rightarrow D\pi$  and  $D^* \rightarrow D^*\pi$  vertices for the upper row read

$$\begin{aligned} v^a(D^* \rightarrow D\pi) &= \frac{g_c}{2f_\pi} \tau_1^a(\boldsymbol{\epsilon}_1 \cdot \mathbf{l}), \\ v^a(D^* \rightarrow D^*\pi) &= \frac{g_c}{2f_\pi} \tau_1^a(-i[\boldsymbol{\epsilon}_1 \times \boldsymbol{\epsilon}'_1] \cdot \mathbf{l}), \end{aligned} \tag{22}$$

where  $\boldsymbol{\epsilon}$  denotes the polarisation vector of the  $D^*$  meson and  $\tau^a$  is the isospin Pauli matrix. Further,  $g_c = 0.57$  is the dimensionless coupling constant which can be extracted from the  $D^* \rightarrow D\pi$  width and  $f_\pi = 92.2$  MeV stands for the pion decay constant.

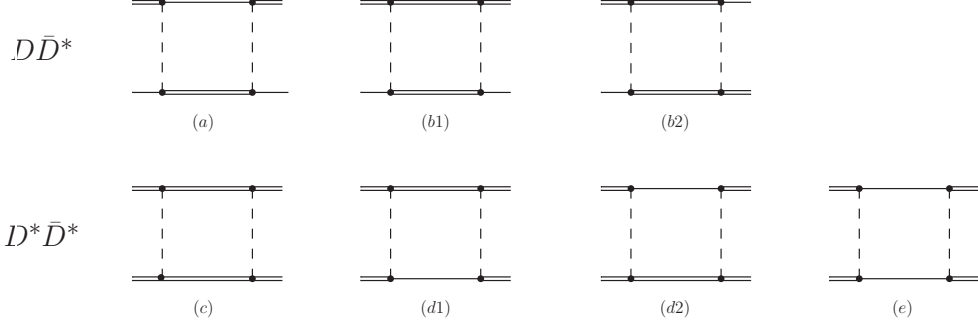


Figure 1: One-loop diagrams which stem from two iterations of the OPE potential: The upper row shows contributions to the  $DD^* \rightarrow DD^*$  transition potential and the lower row is for the  $D^*\bar{D}^* \rightarrow D^*\bar{D}^*$  transition. Single (double) lines are for the  $D$  ( $D^*$ ) mesons and the dashed lines are for the pion.

The amplitudes  $M_i$  ( $i = a, \dots, e$ ) for the diagrams from Fig. 1 can be schematically represented in the form

$$M_i = C \int dl l^2 (\hat{S}L)_i (P_{\pi_1} G(l) P_{\pi_2}), \quad (23)$$

where  $C$  is a numerical coefficient, the same for all diagrams,  $P_{\pi_i}$  ( $i = 1, 2$ ) denote the pion propagators, and  $G$  denotes as before the  $DD$ ,  $DD^*$  or  $D^*\bar{D}^*$  time-ordered perturbation theory (TOPT) propagators, which are identical in all channels in the strict heavy-quark limit. The operator  $(\hat{S}L)_i$  labels the spin-orbit structure of the respective diagram. In particular, the leading divergences from diagrams  $a$  and  $b$  read

$$(\hat{S}L)_a = \int \frac{d\Omega_l}{4\pi} (\boldsymbol{\epsilon}_1 \cdot \mathbf{l})(\boldsymbol{\epsilon}'_1 \cdot \mathbf{l})(\boldsymbol{\epsilon}''_2 \cdot \mathbf{l})(\boldsymbol{\epsilon}''_2 \cdot \mathbf{l}) = \frac{1}{3} l^4 (\boldsymbol{\epsilon}_1 \cdot \boldsymbol{\epsilon}'_1), \quad (24)$$

$$(\hat{S}L)_{b1} = \int \frac{d\Omega_l}{4\pi} (-i[\boldsymbol{\epsilon}_1 \times \boldsymbol{\epsilon}''_1] \cdot \mathbf{l})(-i[\boldsymbol{\epsilon}''_1 \times \boldsymbol{\epsilon}'_1] \cdot \mathbf{l}) l^2 = \frac{2}{3} l^4 (\boldsymbol{\epsilon}_1 \cdot \boldsymbol{\epsilon}'_1), \quad (25)$$

$$(\hat{S}L)_{b2} = \int \frac{d\Omega_l}{4\pi} (-i[\boldsymbol{\epsilon}_1 \times \boldsymbol{\epsilon}''_1] \cdot \mathbf{l})(\boldsymbol{\epsilon}''_1 \cdot \mathbf{l})(\boldsymbol{\epsilon}''_2 \cdot \mathbf{l})(-i[\boldsymbol{\epsilon}''_2 \times \boldsymbol{\epsilon}'_2] \cdot \mathbf{l}) = 0, \quad (26)$$

where, as was explained above, prime (double prime) labels final (intermediate) particles. This yields

$$(\hat{S}L)_{a,b} = (\hat{S}L)_a + (\hat{S}L)_{b1} + (\hat{S}L)_{b2} = l^4 (\boldsymbol{\epsilon}_1 \cdot \boldsymbol{\epsilon}'_1) \quad (27)$$

or, after projecting onto the  ${}^3S_1$  partial waves,

$$(\hat{S}L)_{a,b}({}^3S_1) = l^4 P({}^3S_1)_i P^\dagger({}^3S_1)_i, \quad (28)$$

where we used that the projection operator for the  ${}^3S_1$  partial wave reads for a  $D^*\bar{D}$  state

$$P({}^3S_1)_i = \epsilon_{1i}. \quad (29)$$

		$D\bar{D}$	$D\bar{D}^*$	$D^*\bar{D}^*$			
$1^{++}$	$2^{S+1}L_J$	—	${}^3S_1$ ${}^3D_1$	${}^5D_1$			
	Coeff.	—	1/9 2/9	2/3			
$2^{++}$	$2^{S+1}L_J$	${}^1D_2$	${}^3D_2$	${}^5S_2$ ${}^1D_2$ ${}^5D_2$ ${}^5G_2$			
	Coeff.	2/15	2/5	1/9 2/45 14/45 0			

Table 1: The individual contributions to the coefficients (labelled as Coeff.) in front of the leading divergence in the  $1^{++} D\bar{D}^*({}^3S_1) \rightarrow D\bar{D}^*({}^3S_1)$  and  $2^{++} D^*\bar{D}^*({}^5S_2) \rightarrow D^*\bar{D}^*({}^5S_2)$  one-loop transitions from the intermediate  $D\bar{D}, D\bar{D}^*$  and  $D^*\bar{D}^*$  states in different (allowed) partial waves. Sum over all partial wave contributions is equal to 1 in both channels in agreement with Eqs. (28) and (34).

Similarly, for diagrams  $c-e$  one gets

$$\begin{aligned}
(\hat{S}L)_c &= \int \frac{d\Omega_l}{4\pi} (-i[\boldsymbol{\epsilon}_1 \times \boldsymbol{\epsilon}'_1] \cdot \mathbf{l})(-i[\boldsymbol{\epsilon}''_1 \times \boldsymbol{\epsilon}'_1] \cdot \mathbf{l})(-i[\boldsymbol{\epsilon}_2 \times \boldsymbol{\epsilon}''_2] \cdot \mathbf{l})(-i[\boldsymbol{\epsilon}''_2 \times \boldsymbol{\epsilon}'_2] \cdot \mathbf{l}) \\
&= \frac{l^4}{15} \{6(\boldsymbol{\epsilon}_1 \cdot \boldsymbol{\epsilon}'_1)(\boldsymbol{\epsilon}_2 \cdot \boldsymbol{\epsilon}'_2) + (\boldsymbol{\epsilon}_1 \cdot \boldsymbol{\epsilon}_2)(\boldsymbol{\epsilon}'_1 \cdot \boldsymbol{\epsilon}'_2) + (\boldsymbol{\epsilon}_1 \cdot \boldsymbol{\epsilon}'_2)(\boldsymbol{\epsilon}'_1 \cdot \boldsymbol{\epsilon}_2)\}, \tag{30}
\end{aligned}$$

$$\begin{aligned}
(\hat{S}L)_{d1} &= \int \frac{d\Omega_l}{4\pi} (-i[\boldsymbol{\epsilon}_1 \times \boldsymbol{\epsilon}'_1] \cdot \mathbf{l})(-i[\boldsymbol{\epsilon}''_1 \times \boldsymbol{\epsilon}'_1] \cdot \mathbf{l})(\boldsymbol{\epsilon}_2 \cdot \mathbf{l})(\boldsymbol{\epsilon}'_2 \cdot \mathbf{l}) = \\
&= \frac{l^4}{15} \{4(\boldsymbol{\epsilon}_1 \cdot \boldsymbol{\epsilon}'_1)(\boldsymbol{\epsilon}_2 \cdot \boldsymbol{\epsilon}'_2) - (\boldsymbol{\epsilon}_1 \cdot \boldsymbol{\epsilon}_2)(\boldsymbol{\epsilon}'_1 \cdot \boldsymbol{\epsilon}'_2) - (\boldsymbol{\epsilon}_1 \cdot \boldsymbol{\epsilon}'_2)(\boldsymbol{\epsilon}'_1 \cdot \boldsymbol{\epsilon}_2)\}, \tag{31}
\end{aligned}$$

$$\begin{aligned}
(\hat{S}L)_e &= \int \frac{d\Omega_l}{4\pi} (\boldsymbol{\epsilon}_1 \cdot \mathbf{l})(\boldsymbol{\epsilon}'_1 \cdot \mathbf{l})(\boldsymbol{\epsilon}_2 \cdot \mathbf{l})(\boldsymbol{\epsilon}'_2 \cdot \mathbf{l}) \\
&= \frac{l^4}{15} \{(\boldsymbol{\epsilon}_1 \cdot \boldsymbol{\epsilon}'_1)(\boldsymbol{\epsilon}_2 \cdot \boldsymbol{\epsilon}'_2) + (\boldsymbol{\epsilon}_1 \cdot \boldsymbol{\epsilon}_2)(\boldsymbol{\epsilon}'_1 \cdot \boldsymbol{\epsilon}'_2) + (\boldsymbol{\epsilon}_1 \cdot \boldsymbol{\epsilon}'_2)(\boldsymbol{\epsilon}'_1 \cdot \boldsymbol{\epsilon}_2)\}, \tag{32}
\end{aligned}$$

and  $(\hat{S}L)_{d2} = (\hat{S}L)_{d1}$ , since the diagrams  $d1$  and  $d2$  differ from each other only by an index permutation for the intermediate particles. Summing up the individual contributions given above one arrives at

$$(\hat{S}L)_{c,d,e} = l^4(\boldsymbol{\epsilon}_1 \cdot \boldsymbol{\epsilon}'_1)(\boldsymbol{\epsilon}_2 \cdot \boldsymbol{\epsilon}'_2) \tag{33}$$

or, after projecting onto the  ${}^5S_2$  partial waves,

$$(\hat{S}L)_{c,d,e}({}^5S_2) = l^4 P({}^5S_2)_{ij} P({}^5S_2)_{ij}^\dagger, \tag{34}$$

where the  ${}^5S_2$  projector has the form

$$P({}^5S_2)_{ij} = \frac{1}{2} \left( \epsilon_{1i}\epsilon_{2j} + \epsilon_{1j}\epsilon_{2i} - \frac{2}{3}\delta_{ij}(\boldsymbol{\epsilon}_1 \cdot \boldsymbol{\epsilon}_2) \right). \tag{35}$$

By comparing the coefficients in front of the leading divergences in Eqs. (28) and (34), one can see that they indeed coincide. This should not come as a surprise, given that, in the spin-symmetry limit, there is only one contact term available in the investigated transitions. It should be noted that, as soon as one of the external angular momenta is a  $D$  wave, some momenta in the pion exchange amplitudes need to be identified with the external momenta

in order to construct a  $D$ -wave projector. This reduces the degree of divergence of the corresponding integrals thus making them convergent.

It is important to emphasise that the discussed equality of the leading divergences in the  $D^*\bar{D}$  and  $D^*\bar{D}^*$  channels—see Eqs. (28) and (34)—comes as a result of a delicate interplay between the contributions from different partial waves and different channels, as illustrated in Table 1. For example, neglecting any  $D$ -wave in the intermediate state destroys this equality, although  $D$  waves still can be neglected altogether. Also, this equality is destroyed if any of the diagrams in Fig. 1 is neglected (except for the diagram  $b2$  which does not contribute to the leading divergence). In particular, in Ref. [24] OPE is included only for the diagonal transitions  $D\bar{D}^* \rightarrow D\bar{D}^*$  and  $D^*\bar{D}^* \rightarrow D^*\bar{D}^*$  while the coupled-channel dynamics is neglected altogether. This implies that diagrams  $b1$ ,  $b2$ ,  $d1$ ,  $d2$ , and  $e$  are dropped in this work. However, this approximation leads to a violation of HQSS since the retained diagrams  $a$  and  $c$  have different coefficients in front of the leading divergence. Indeed, as can be seen from Table 1, neglecting the  $D^*\bar{D}^*$  intermediate states in the  $1^{++}$  channel leads to the coefficient  $1/3$  which is associated with diagram  $a$  while neglecting the  $DD$  and  $D\bar{D}^*$  intermediate states in the  $2^{++}$  channel results in the coefficient  $7/15$  corresponding to diagram  $c$ . Hence, the single contact term present in the heavy-quark limit cannot absorb the divergences in the  $1^{++}$  and  $2^{++}$  channels simultaneously. As a consequence, the results of the pionfull calculations of Ref. [24] should reveal some cutoff dependence.

One more comment on the sum over partial waves in the intermediate states is in order here. An explicit calculation in the partial wave basis shows that diagram  $b1$  in Fig. 1 acquires a contribution from the intermediate  ${}^3S_1$  partial wave which is, however, in contradiction with the required positive C-parity of the  $D^*\bar{D}^*$  pair. Interestingly, the same contribution but with the opposite sign appears from diagram  $b2$ , although the net result from this diagram is zero—see Eq. (26). This can be understood as follows: diagram  $b1$  contains the sum of a contribution with positive C-parity and a contribution with negative C-parity while diagram  $b2$  contains their difference. Therefore the sum of diagrams  $b1$  and  $b2$  restores the required positive C-parity of the corresponding loop contribution while, at the same time, the UV-piece of diagram  $b2$  vanishes since, in this limit, the contributions from different partial waves cancel. This demonstrates that, although diagram  $b2$  does not contribute to the UV-divergent piece of the one-loop amplitude, its omission has still to be done with caution to avoid problems with the C-parity of the amplitude.

Notice that the power of divergence of the one-loop integrals for the diagrams in Fig. 1 depends on the form of the  $D^{(*)}\bar{D}^{(*)}$  propagator  $G$ . In this work we use nonrelativistic propagators, so that the one-loop contributions diverge linearly<sup>3</sup> and higher powers of divergences show up starting from the third iteration of OPE. Then we choose the cutoff in the Lippmann-Schwinger-type equations of the order of a natural hard scale in the problem—see, for example, Refs. [34–36] in the context of nuclear EFT. Alternatively, if one uses a relativised propagator  $G$ , all iterations of OPE produce only logarithmic divergences which can be absorbed altogether by a single contact term for any value of the cutoff [37]; see also Ref. [38] for the related work in the nucleon-nucleon problem. However, since the physical results should not depend on the particular method used, we here stick to the nonrelativistic propagator.

---

<sup>3</sup>One might be tempted to argue that in dimensional regularisation power divergences vanish. However, this is a scheme-dependent result which should be interpreted with caution, as discussed in detail in Ref. [33].

### 3.2. Strict heavy-quark limit: nonperturbative inclusion of the OPE interactions

We are now in the position to include the OPE interaction beyond one loop. Following the logic developed in the previous section, we start from the strict heavy-quark limit. Unlike the  $S$ -wave contact interactions, OPE allows for transitions to heavy-meson states in higher partial waves which have therefore to be included in an extended set of basis states,

$$\begin{aligned}
0^{++} &: \{D\bar{D}(^1S_0), D^*\bar{D}^*(^1S_0), D^*\bar{D}^*(^5D_0)\}, \\
1^{+-} &: \{D\bar{D}^*(^3S_1, -), D\bar{D}^*(^3D_1, -), D^*\bar{D}^*(^3S_1), D^*\bar{D}^*(^3D_1)\}, \\
1^{++} &: \{D\bar{D}^*(^3S_1, +), D\bar{D}^*(^3D_1, +), D^*\bar{D}^*(^5D_1)\}, \\
2^{++} &: \{D\bar{D}(^1D_2), D\bar{D}^*(^3D_2), D^*\bar{D}^*(^5S_2), D^*\bar{D}^*(^1D_2), D^*\bar{D}^*(^5D_2), D^*\bar{D}^*(^5G_2)\},
\end{aligned} \tag{36}$$

where, as before the C parity of the state is indicated explicitly in parenthesis whenever necessary.

The integral equations for the scattering amplitude can be written as

$$a_{ik}^{(JPC)}(p, p') = V_{ik}^{(JPC)}(p, p') - \sum_j \int dk k^2 V_{ij}^{(JPC)}(p, k) G_j(k) a_{jk}^{(JPC)}(k, p'), \tag{37}$$

where  $i, j$  and  $k$  label the basis vectors in the order they appear in Eq. (36). As before all propagators  $G_j$  are equal in the heavy-quark limit.

Performing a unitarity transformation on the basis states given in Eqs. (36), one arrives at

$$\tilde{a}_{ik}^{(JPC)}(p, p') = \tilde{V}_{ik}^{(JPC)}(p, p') - \sum_j \int dk k^2 \tilde{V}_{ij}^{(JPC)}(p, k) G_j(k) \tilde{a}_{jk}^{(JPC)}(k, p'), \tag{38}$$

where  $\tilde{a}^{(JPC)} = U^{(JPC)} a^{(JPC)} U^{(JPC)\dagger}$  and  $\tilde{V}^{(JPC)} = U^{(JPC)} V^{(JPC)} U^{(JPC)\dagger}$ . For a given set of quantum numbers  $\{JPC\}$  one can find the operator  $U^{(JPC)}$  such that the transformed potentials take a block-diagonal form (for the sake of transparency, the size of the blocks is quoted explicitly in parenthesis),

$$\begin{aligned}
\tilde{V}^{(0^{++})}(3 \times 3) &= A(2 \times 2) \oplus B(1 \times 1), \\
\tilde{V}^{(1^{+-})}(4 \times 4) &= A(2 \times 2) \oplus B(1 \times 1) \oplus C(1 \times 1), \\
\tilde{V}^{(1^{++})}(3 \times 3) &= A(2 \times 2) \oplus D(1 \times 1), \\
\tilde{V}^{(2^{++})}(6 \times 6) &= A(2 \times 2) \oplus D(1 \times 1) \oplus E(3 \times 3).
\end{aligned} \tag{39}$$

The OPE contributes to all five submatrices,  $A$ ,  $B$ ,  $C$ ,  $D$ , and  $E$ , while the contact interaction contributes only to matrix  $A$  (in the form of the linear combination  $C_0 = C_{0a} + C_{0b}$ ) and to matrix  $B$  (as the linear combination  $C'_0 = C_{0a} - 3C_{0b}$ ). Accordingly, matrices  $C$ ,  $D$ , and  $E$  do not contain  $S$ -wave-to- $S$ -wave transitions and are therefore quite unlikely to bring about bound states. Since matrix  $A$  enters all four potentials in Eq. (39) simultaneously, the degenerate bound states controlled by the contact potential  $C_0$  appear in all four channels as before and, again as before, two additional degenerate bound states may exist in the channels  $0^{++}$  and  $1^{+-}$ . They come from matrix  $B$  and are controlled by the contact interaction  $C'_0$ .

We therefore observe that the specific pattern of degenerate bound states found in the purely contact theory survives the inclusion of the OPE interaction. Meanwhile, in line with

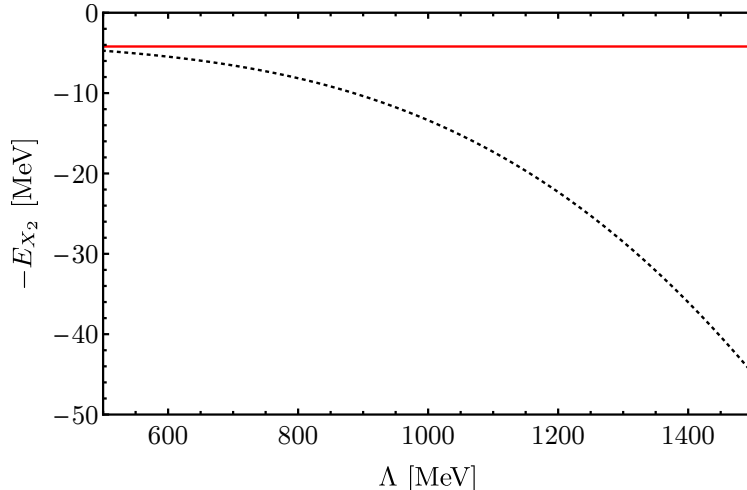


Figure 2: The binding energy of the  $2^{++}$  spin partner of the  $X(3872)$  in the strict heavy-quark limit: Red solid line—all coupled-channel transitions are included,  $E_{X_2} = E_X = 4.2$  MeV; black dashed line—particle coupled-channel transitions in the potentials  $D\bar{D}^* \rightarrow D\bar{D}^*$  and  $D^*\bar{D}^* \rightarrow D^*\bar{D}^*$  driven by the OPE interaction are neglected.

the considerations of the previous subsection, we emphasise that the irreducible decomposition discussed above leads to degenerate states only if the basis vectors as given in Eqs. (36) are included consistently. Specifically, the states remain degenerate if *all*  $D$ -wave-to- $D$ -wave transitions are dropped in all coupled channels or/and if *all*  $S$ - $D$  transitions are dropped.<sup>4</sup> However, neglecting the particle coupled-channel dynamics or some higher partial waves immediately destroys the degeneracy deduced from the HQSS and leads to cutoff-dependent results for the partner states, since the cancellation of the divergences appears as a result of a delicate interplay between different partial wave amplitudes, as explained in the previous subsection. To illustrate this issue, in Fig. 2, we show the cutoff dependence of the binding energy  $E_{X_2}$  of the  $2^{++}$  spin partner of the  $X(3872)$  in the strict heavy-quark limit. The arguments given above predict that  $E_{X_2}$  takes exactly the same value as the binding energy of the  $X(3872)$  for which we stick to the value used in Ref. [24] for the isospin limit, namely  $E_X = 4.2$  MeV. In addition,  $E_{X_2}$  should reveal no cutoff dependence. This is indeed the case for the full calculation—see the red solid line in Fig. 2. On the other hand, neglecting the particle coupled-channel transitions in the potentials  $D\bar{D}^* \rightarrow D\bar{D}^*$  and  $D^*\bar{D}^* \rightarrow D^*\bar{D}^*$  governed by the OPE interaction results in strongly cutoff-dependent predictions—see the dashed black line in Fig. 2. This approximation was used in Ref. [24] to predict the HQSS partner of the  $X(3872)$ . Meanwhile, a quantitative comparison of the results contained in the aforementioned papers with those presented in Fig. 2 is not straightforward since (i) the result from Fig. 2 is obtained in the strict HQSS limit while in Ref. [24] the effects beyond the heavy-quark limit are also included and (ii) different regularisation schemes were used: a rather soft exponential regulator of the form  $\exp(-p^2/\Lambda^2)$  with  $\Lambda = 0.5$  and 1 GeV in Ref. [24] versus a sharp cutoff employed in this work.

<sup>4</sup>Note that transitions involving the  $G$ -wave contribute only to the matrix  $E(3 \times 3)$  and are therefore irrelevant for the formation of the discussed degenerate bound states in the heavy-quark limit.

### 3.3. Beyond leading order

As discussed above, the leading correction to the results obtained in the strict HQSS limit comes from the  $D^*$ - $D$  mass difference that we denote as  $\delta$ —see Eq. (15). The probably most spectacular new effect that comes into the system when both OPE and the leading corrections in  $\delta$  are taken into account simultaneously is the finite width of the  $2^{++}$   $D^*\bar{D}^*$  state that can now decay into the  $^1D_2$   $D\bar{D}$  pair. Within a theory with perturbative pions, in Ref. [26], this width was estimated to lie in the range from just a few units to about a dozen MeV depending on a particular model used for the pion form factor—see Table I of Ref. [26]. Here we investigate for the first time the effect in a theory with nonperturbative pions.

We expect the nonperturbative pion dynamics to be especially relevant for the transitions at hand since the momentum of the  $D$  and  $\bar{D}$  mesons in the final state that emerges from a shallow  $D^*\bar{D}^*$  bound state is about

$$q_1 = \sqrt{2\mu(2\delta)} \approx 700 \text{ MeV}. \quad (40)$$

Transitions from the  $D^*\bar{D}^*$  system to the  $D\bar{D}$  final state also provide some inelasticity and here the relevant momenta, of the order of

$$q_2 = \sqrt{2\mu_*\delta} \approx 500 \text{ MeV}, \quad (41)$$

are quite sizeable as well. In particular, both momenta are significantly larger than the pion mass. A direct consequence of this is that  $D$  waves fed by the OPE are not subject to a kinematic suppression relative to the  $S$  waves.

In order to calculate the observables, we proceed stepwise:

- Our leading-order potential consists of the low-energy constant  $C_0$ , adjusted to reproduce the  $X(3872)$  binding energy, and the static OPE potential (see Refs. [24, 31] and, in particular, Appendix C of Ref. [24] for the explicit expressions which we reproduce). In order to connect to the results of Ref. [24] more directly, the  $X(3872)$  binding energy is chosen to be  $E_X = 4.2$  MeV.
- The Green's functions  $G_i$  ( $i = D\bar{D}, D\bar{D}^*, D^*\bar{D}^*$ ) in Eq. (37) contain now the physical masses of the  $D$  and  $D^*$  mesons and in this way introduce into the system the intermediate momentum scales  $q_1$  and  $q_2$ , defined in Eqs. (40) and (41), respectively.
- The differential production rate  $d\text{Br}/dE$ , as a function of the energy  $E$  counted relative to the  $D^*\bar{D}^*$  threshold, is calculated from the convolution of the amplitude with a pointlike source,

$$\frac{d\text{Br}}{dE} = \text{const} \times |J(E)|^2 k, \quad J(E) = \int dq q^2 \frac{a_{D^*\bar{D}^* \rightarrow D\bar{D}}(q, k, E)}{E - q^2/m_* + i0}, \quad (42)$$

where  $k = \sqrt{m(2\delta + E)}$  denotes the  $D\bar{D}$  two-body phase space and  $a_{D^*\bar{D}^* \rightarrow D\bar{D}}(q, k, E)$  denotes the solution of the coupled channel scattering Eq. (37) in the half off-shell kinematics.

The function  $J(E)$  has a clear Breit-Wigner shape that allows one to extract the (binding) energy and the width of the resonance from the shape of the below-threshold peak describing the  $2^{++} D^* \bar{D}^*$  bound state. These quantities are shown in Fig. 3 as functions of the cutoff used to regularise the Lippmann-Schwinger equations. To assess the sensitivity of the results obtained to the form of the regulator we used two different regularisation schemes: the sharp cutoff  $\theta(\Lambda - p)$  (the solid curves in Fig. 3) and the exponential function  $\exp(-p^6/\Lambda^6)$  (the dashed curves in Fig. 3). Since we treat the momenta  $q_1$  and  $q_2$ , defined in Eqs. (40) and (41), as soft scales, it is important to use a regulator that does not cut the momenta of their order. Both regulators mentioned above meet this criterion and lead to quite similar results for the parameters of the  $X_2$  bound state, as seen from Fig. 3. The cutoff in the calculation is chosen to be of the order of the hard scale of the problem which is expected to be larger than  $q_1$  but should not be taken too large to appropriately renormalise the scattering amplitude in the nonperturbative calculations [34, 35]. We therefore let the cutoff vary in the range 800-1500 MeV. Such a conservatively chosen cutoff range allows us to estimate more reliably the impact of higher-order HQSS violating contact operators on the nonperturbative results. In particular, as will be seen below, the  $\Lambda$ -dependence of the results remains moderate even if one approaches larger values of the cutoff. For smaller cutoffs the separation of the soft and hard scales becomes worse and the results for the binding energy reveal larger dependence on the cutoff and on the choice of the regularisation scheme.

From the results presented in Fig. 3 one is led to conclude that the scales emerging in the coupled-channel approach due to the nonperturbative treatment of the pions generate a significant shift of the  $2^{++}$  spin partner of the  $X(3872)$  and make it as broad as 40-60 MeV. Those values are a few times to an order of magnitude larger than predicted in Ref. [26].<sup>5</sup> However, these findings have to be interpreted with caution. As was discussed in Subsec. 2.2, proceeding beyond the strict HQSS limit requires the presence of an extra counter term to absorb the cutoff dependence of the results. In the spirit of the numerical implementation of the renormalisation group equations, the residual  $\Lambda$ -dependence of the parameters of the  $X_2$  bound state found for the cutoff varied in a reasonable range—see Fig. 3—provides a rough estimate of the importance of such a counter term. From the right plot in Fig. 3 one can see that the observed dependence of  $\Gamma_{X_2}$  on  $\Lambda$  is quite mild even when  $\Lambda$  approaches the mass of the  $D$ -meson, where corrections to the heavy-quark limit could become significant. This appears to be in line with the discussion in the end of Subsec. 2.2 where a similar observation was made for a purely contact theory beyond the HQSS limit. Therefore, the conclusion on the broadening of the  $X_2$  state may be treated as a reliable prediction of the approach used in this work. The discrepancy between this result and the conclusions of the previous study in Ref. [26] should be ascribed to the fact that in the latter work the  $D$ -wave contributions were suppressed by construction, since pions were included perturbatively. Contrary to this there is no suppression of the  $D$  waves in our approach.

Meanwhile, the dependence of the binding energy  $E_{X_2}$  on the value of the cutoff  $\Lambda$  as well as on the regulator employed (left plot in Fig. 3) appears to be quite strong. In addition, the large momentum scales  $q_1$  and  $q_2$  call for an extension of the model in order to incorporate further effects important for the problem. In particular, other members of the SU(3) pseudo-scalar octet and probably the vector mesons, whose masses are comparable with the relevant

---

<sup>5</sup>We also checked by an explicit calculation that similar values of the parameters can be extracted from the differential rate of the two-step production process  $D^* \bar{D}^* \rightarrow D \bar{D}^* \rightarrow D \bar{D} \pi$  from a pointlike source.

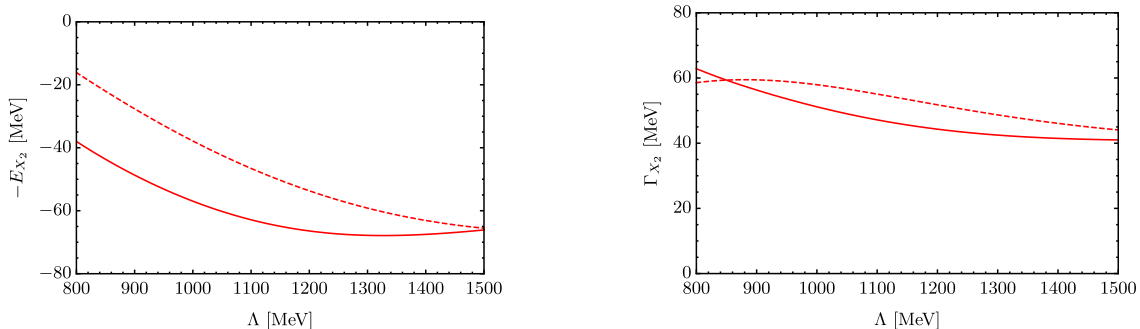


Figure 3: The energy and the width of the  $2^{++}$  bound  $D^*\bar{D}^*$  state extracted using a Breit-Wigner parameterisation from the shape of the production rate, Eq. (42), as functions of the cutoff  $\Lambda$  using two different regularisation schemes in the Lippmann-Schwinger equations : i) sharp cutoff (solid lines), ii) the exponential regularisation of the form  $f(p) = \exp(-p^6/\Lambda^6)$  (dashed lines).

scales in the system at hand, should be included. In addition, three-body effects related to the  $D\bar{D}\pi$  dynamics may also play a role and should be included—see Refs. [37, 39, 40] for the earlier works on the  $X(3872)$  using nonperturbative pions and Refs. [41, 42] for the works including pions perturbatively. Therefore, while the results of our calculations indicate that the  $X_2$  state is shifted downwards in mass as soon as the leading HQSS violating effects are included, we are not able at present to quantify this effect reliably. However, as argued above, our estimate for the width of the  $X_2$  in the range  $50 \pm 10$  MeV from nonperturbative pions remains to be a stable prediction of our approach as the variation of the width with the cutoff is small compared to the width itself—see the right plot in Fig. 3.

#### 4. Conclusions and outlook

In this paper we investigated the role of the pion exchange interactions for the formation of the spin partners of the molecular state  $X(3872)$ . We demonstrated explicitly that the inclusion of the OPE interactions does not spoil the results of the pure contact theory in the strict heavy-quark limit which predicts the existence of 3 degenerate spin partners of the  $1^{++}$  state  $X(3872)$  with the quantum numbers  $0^{++}$ ,  $1^{+-}$  and  $2^{++}$ . However, we found that this conclusion as well as other predictions of the effective field theory incorporating both the contact and the OPE interactions can be regarded as reliable if, and only if, all particle coupled-channel effects and all relevant partial waves for the pion-exchange potential are taken into account. We demonstrated analytically to one-loop order that any omission of these requirements results in a violation of the heavy-quark spin symmetry. We further confirmed this observation by an explicit nonperturbative numerical calculation of the  $X(3872)$  spin-2 partner binding energy  $E_{X_2}$  in the strict heavy-quark limit: once the relevant low-energy constant is fixed to reproduce the mass of the  $X(3872)$  for any given value of the cutoff  $E_{X_2}$  turns out to be independent of  $\Lambda$  in the full model. On the contrary, neglecting the  $D\bar{D}$  and/or  $D\bar{D}^*$  coupled-channel effects (in the  $D$  waves) we find a strong cutoff dependence of  $E_{X_2}$  even in the strict HQSS limit.

Proceeding beyond the HQSS limit brings the scale  $\delta$ —the  $D^*-D$  mass difference. This results in new effects caused by the coupled-channel dynamics. In particular, in case of the spin partners with the quantum numbers  $0^{++}$  and  $1^{+-}$  the spin-symmetry-violating terms in the heavy meson-antimeson propagators lift the degeneracy argued for in the symmetry

limit and make each pole sensitive to the strength of both leading-order low-energy constants individually and not only to their sum which may be fixed from the mass of the  $X(3872)$ .

In addition, we observe that, even without coupled channels, already the leading spin-symmetry violating contribution calls for an additional counter term for the  $D^{(*)}\bar{D}^{(*)}$  scattering system in order to absorb the dependence of the results on the regulator. This might put into question the possibility of an accurate prediction of the spin partners of the  $X(3872)$ . We demonstrate by an explicit calculation that it is still possible to at least estimate both the binding energy and the width for the spin partner of the  $X(3872)$  with the quantum numbers  $2^{++}$ . For this we performed a coupled-channel analysis of the  $D^*\bar{D}^*$  state with these quantum numbers and found that the coupled-channel effects in the effective field theory incorporating both the contact and the OPE interactions had a strong impact on the parameters of this state and resulted in a sizable shift of the corresponding pole of the scattering matrix. In particular, we found that the binding energy and the width of this spin-2 partner of the  $X(3872)$  both appeared to be of the order of several dozens MeV, that is significantly larger compared to the values found in the literature. We argue that, while the increase of the  $X_2$  binding energy can only be viewed as a qualitative result the conclusion on the broadening of the  $X_2$  is related to unitarity and therefore is a reliable prediction of our approach.

We emphasise that further progress and the possibility of more accurate predictions for the partner states should rely on a study of the convergence pattern of the approach used and in particular on an estimate of the role of higher-order contact interactions with two derivatives. Although these terms are formally suppressed in chiral EFT they might appear relevant here due to the relatively large momenta involved in the problem—see Eqs. (40) and (41). In addition, a more sophisticated study should include the three-body scales related to the  $D\bar{D}\pi$  dynamics and an investigation of the role of the other members of the SU(3) pseudoscalar octet and vector mesons, whose masses are comparable with the scales relevant for the problem.

We are grateful to F.-K. Guo, J. Nieves and M. P. Valderrama for useful comments on the manuscript. This work is supported in part by the DFG and the NSFC through funds provided to the Sino-German CRC 110 “Symmetries and the Emergence of Structure in QCD” (NSFC Grant No. 11261130311). A. N. acknowledges support from the Russian Science Foundation (Grant No. 15-12-30014). Work of V. B. is supported by the DFG (Grant No. GZ: BA 5443/1-1). The work of UGM was also supported by the CAS President’s International Fellowship Initiative (PIFI) (Grant No. 2015VMA076).

## References

- [1] N. Brambilla *et al.*, Eur. Phys. J. C **71** (2011) 1534.
- [2] S. Eidelman, Acta Phys. Polon. B **47** (2016) 109.
- [3] S. K. Choi *et al.* [Belle Collaboration], Phys. Rev. Lett. **91** (2003) 262001.
- [4] K. A. Olive *et al.* [Particle Data Group Collaboration], Chin. Phys. C **38** (2014) 090001.
- [5] M. B. Voloshin and L. B. Okun, JETP Lett. **23** (1976) 333 [Pisma Zh. Eksp. Teor. Fiz. **23** (1976) 369].
- [6] A. De Rujula, H. Georgi and S. L. Glashow, Phys. Rev. Lett. **38** (1977) 317.
- [7] N. A. Tornqvist, Phys. Lett. B **590** (2004) 209.
- [8] N. A. Tornqvist, Phys. Rev. Lett. **67** (1991) 556.
- [9] E. S. Swanson, Phys. Lett. B **588** (2004) 189.
- [10] C. Y. Wong, Phys. Rev. C **69** (2004) 055202.

- [11] C. Hanhart, Yu. S. Kalashnikova, A. E. Kudryavtsev and A. V. Nefediev, Phys. Rev. D **76** (2007) 034007.
- [12] R. Aaij *et al.* [LHCb Collaboration], Phys. Rev. Lett. **110** (2013) 222001.
- [13] T. Barnes, S. Godfrey and E. S. Swanson, Phys. Rev. D **72** (2005) 054026.
- [14] R. Faccini, A. Pilloni and A. D. Polosa, Mod. Phys. Lett. A **27** (2012) 1230025.
- [15] F. E. Close and P. R. Page, Phys. Lett. B **578** (2004) 119.
- [16] M. Suzuki, Phys. Rev. D **72** (2005) 114013.
- [17] Yu. S. Kalashnikova, Phys. Rev. D **72** (2005) 034010.
- [18] I. V. Danilkin and Yu. A. Simonov, Phys. Rev. Lett. **105** (2010) 102002.
- [19] C. Hidalgo-Duque, J. Nieves, A. Ozpineci and V. Zamiralov, Phys. Lett. B **727** (2013) 432.
- [20] M. Cleven, F. K. Guo, C. Hanhart, Q. Wang and Q. Zhao, Phys. Rev. D **92** (2015), 014005.
- [21] A. E. Bondar, A. Garmash, A. I. Milstein, R. Mizuk and M. B. Voloshin, Phys. Rev. D **84** (2011) 054010
- [22] M. B. Voloshin, Phys. Rev. D **84** (2011) 031502
- [23] T. Mehen and J. W. Powell, Phys. Rev. D **84** (2011) 114013.
- [24] J. Nieves and M. P. Valderrama, Phys. Rev. D **86** (2012) 056004.
- [25] F. K. Guo, C. Hidalgo-Duque, J. Nieves and M. P. Valderrama, Phys. Rev. D **88** (2013) 054007.
- [26] M. Albaladejo, F.-K. Guo, C. Hidalgo-Duque, J. Nieves and M. P. Valderrama, Eur. Phys. J. C **75** (2015), 547.
- [27] E. Cincioglu, J. Nieves, A. Ozpineci and A. U. Yilmazer, Eur. Phys. J. C **76** (2016), 576.
- [28] I. K. Hammer, C. Hanhart and A. V. Nefediev, arXiv:1607.06971 [hep-ph].
- [29] F.-K. Guo, C. Hanhart, Y. S. Kalashnikova, P. Matuschek, R. V. Mizuk, A. V. Nefediev, Q. Wang and J.-L. Wymen, Phys. Rev. D **93** (2016), 074031.
- [30] M. T. AlFiky, F. Gabbiani and A. A. Petrov, Phys. Lett. B **640** (2006) 238.
- [31] M. P. Valderrama, Phys. Rev. D **85** (2012) 114037.
- [32] C. Hidalgo-Duque, J. Nieves and M. P. Valderrama, Phys. Rev. D **87** (2013) 076006.
- [33] V. Baru, E. Epelbaum, A. A. Filin, F.-K. Guo, H.-W. Hammer, C. Hanhart, U.-G. Meißner and A. V. Nefediev, Phys. Rev. D **91** (2015) 034002.
- [34] G. P. Lepage, nucl-th/9706029.
- [35] E. Epelbaum and U.-G. Meißner, Few Body Syst. **54**, (2013) 2175.
- [36] A. Nogga, R. G. E. Timmermans, and U. van Kolck, Phys. Rev. C **72**, (2005) 054006.
- [37] V. Baru, E. Epelbaum, A. A. Filin, J. Gegelia and A. V. Nefediev, Phys. Rev. D **92** (2015) no.11, 114016.
- [38] E. Epelbaum and J. Gegelia, Phys. Lett. B **716**, (2012) 338.
- [39] V. Baru, E. Epelbaum, A. A. Filin, C. Hanhart, U.-G. Meißner and A. V. Nefediev, Phys. Lett. B **726** (2013) 537.
- [40] V. Baru, A. A. Filin, C. Hanhart, Yu. S. Kalashnikova, A. E. Kudryavtsev and A. V. Nefediev, Phys. Rev. D **84** (2011) 074029.
- [41] S. Fleming, M. Kusunoki, T. Mehen and U. van Kolck, Phys. Rev. D **76** (2007) 034006.
- [42] M. Jansen, H.-W. Hammer and Y. Jia, Phys. Rev. D **92** (2015) 114031.